Corrosion of femtosecond laser surface textured aluminium alloy

Ley, James R.; Kwon, Young W.; Park, Chanman; Menon, Sarath K.

Institute of Materials, Minerals and Mining (IMMM)

Ley, James R., et al. "Corrosion of femtosecond laser surface textured aluminium alloy." Corrosion Engineering, Science and Technology 52.7 (2017): 526-532. http://hdl.handle.net/10945/66180

CORROSION ENGINEERING, SCIENCE AND TECHNOLOGY, 2017
https://doi.org/10.1080/1478422X.2017.1348090

The Institute of Materials, Minerals and Mining

Taylor & Francis
Taylor & Francis Group

Corrosion of femtosecond laser surface textured aluminium alloy

James R. Ley, Young W. Kwon, Chanman Park and Sarath K. Menon

Department of Mechanical & Aerospace Engineering, Naval Postgraduate School, Monterey, CA, USA

ABSTRACT

With superhydrophobic properties being extended to a variety of metallic substrates through the process of ablation due to femtosecond laser surface processing (FLSP), it is important to understand corrosion behaviour of such a processed material. The material was tested through the use of an accelerated corrosion fog chamber using both treated and untreated aluminium alloy samples. During the accelerated corrosion testing, the FLSP-treated sample suffered from pitting corrosion at a rate faster than the untreated sample, effectively removing the surface treatment. While there are significant hydrodynamic benefits to this material, the elevated corrosion rates raise concerns about the resiliency of this surface treatment.

ARTICLE HISTORY
Received 30 March 2017
Accepted 23 June 2017

KEYWORDS
Accelerated corrosion; femtosecond laser; superhydrophobic; superhydrophilic

Introduction

In an economically driven world, great emphasis is always placed on engineers to design a system that is the most efficient; it can be without sacrificing its intended purpose to reduce operating costs. The U.S. Navy spends millions of dollars a year in operational costs such as fuel, corrosion prevention, and biofouling remediation [1]. In an attempt to reduce operating costs, there has been a continuous search for new methods and materials to increase the efficiency of current systems. One such material of particular interest for the U.S. Navy's aqueous environment is one that exhibits superhydrophobic properties.

A material is classified as superhydrophobic if the contact angle of a water droplet is larger than 150° and the contact hysteresis angle is less than 10° [2]. The superhydrophobic properties were observed on the lotus leaf [3]. From the observation, it was found that the micro-scale surface roughness contributes to hydrophobicity [4]. As a result, there have been attempts to modify the surfaces on both micro-scale and nano-scale. Initially, the photolithography technique was used to create structures on silicon wafers such as nano-grass and nanobricks [5]. These structures were later coated with a thin CF_x film by plasma vapour deposition to obtain the desired superhydrophobic properties. The silicon wafers were then assembled into a rectangular form and submerged in a water tunnel for flow testing, the results of which showed a significant reduction in drag at all fluid velocities tested, and as much as 50% in the laminar region. Another study used a lithographic process to produce silicon wafer moulds in which polydimethylsiloxane (PDMS) was cast into 150 mm long patches, and then seamlessly joined to create a 1 m long superhydrophobic surface [6]. Additionally, polymer-based micro- and nano-scaled chemical coatings were used [7].

More recently, the femtosecond laser surface processing (FLSP) technique was applied to functionalise the surface of metallic surfaces through ablation [8,9]. This technique can produce nano-scale or micro-scale roughness on metallic materials. They could create both superhydrophobic and superhydrophilic properties on metallic surfaces. With increasing fluence came an increase in average surface roughness. It was also noted that samples directly after surface processing exhibited superhydrophilic properties with contact angles less than 20°. However, when the samples were allowed to rest in normal atmosphere, or in a carbon dioxide-rich atmosphere, it was noted that soon after surface properties exhibited hydrophobic or superhydrophobic characteristics. The length of time required for the change in properties is proportional to the fluence. After performing elemental surface analysis (XPS) to monitor the change in surface chemistry following functionalisation, it was observed that there was a dramatic increase in the presence of carbon [8]. This was attributed to the creation of a nonstoichiometric oxygen-deficient iron oxide scale (active magnetite, $Fe_3O_{4-\delta}$). The presence of this magnetite caused the catalysation and dissociative absorption of carbon dioxide. Carbon dioxide becomes zero valence carbon monoxide and oxygen anions diffuse into lattice vacancies to form stoichiometric Fe_3O_4. This causes the gradual accumulation of nonpolar carbon on the rough dual scale surface, and in conjunction, create a surface topography that is superhydrophobic.

Owing to the resiliency and durability of metal over silicon structures and polymer coatings, FLSP-functionalised metallic substrates offer a practical engineering material that can be used in commercial applications where superhydrophobic properties are desirable such as reducing drag on the hull of a ship, which, in turn, lowers the amount of fuel consumed.

Some studies have been conducted for corrosion tests on superhydrophobic samples for short-term responses. A study used Al–5%Mg alloy coated using fluoropolymer blend and fumed silica nanoparticles for superhydrophobicity [10] and carried out immersion corrosion tests in seawater for up to 21 days. The study suggested that biofouling in photobiologically active seawater could result in the loss of superhydrophobic coating and increase in the corrosion while pitting corrosion occurred in samples with or without superhydrophobic coating in photobiologically inactive seawater though after 3 weeks, less than 50% of the coating was exfoliated. Another study [11] carried out electrochemical polarisation measurements on an AMG alloy (an Al alloy with

CONTACT Young W. Kwon ywkwon@nps.edu Department of Mechanical & Aerospace Engineering, Naval Postgraduate School, Monterey, CA 93943, USA

3 Mg and other minor alloying elements) processed with nanosecond laser treatment of the surface followed by a superhydrophobic coating in 0.5 M NaCl solution. They demonstrated that though at short exposure times the pitting potential was high, the coating properties deteriorated upon prolonged immersion and the pitting potential approached the corrosion potential in 10 days.

In this study, samples were placed in a salt fog chamber and monitored for the progression of corrosion to determine the resiliency of FLSP functionalisation for the study of long-term effects. Long-term accelerated corrosion exposure tests (ASTM-B117) were carried out in a salt fog chamber for evaluation. Ultimately, the goal of this research is to provide insight into the viability of integrating these materials into areas that would benefit from self-cleaning low hydrodynamic drag applications.

Experiments

To test the resiliency of functionalised surfaces compared to untreated samples with respect to environmental conditions, an accelerated corrosion method was used following ASTM-B117 standards.

Samples

Twenty-one square-shaped samples of 25.4 × 25.4 mm (1 × 1 in.) were obtained from the University of Nebraska-Lincoln. These samples consisted of three groups of seven; each group consisted of superhydrophobic, superhydrophilic, and untreated samples. Each treated sample was prepared with the same FLSP parameters. The laser can produce 1 mJ and 50 fs pulses with up to 1 kHz [12]. The laser power was adjusted for 1.4 J cm^{-2} on the sample surface. The processing was conducted in the room temperature. The differing surface properties were obtained by the environmental conditions to which the samples were exposed directly after laser texturing. As explained above, superhydrophobic samples were exposed to a carbon-rich atmosphere, while superhydrophilic samples were exposed to a carbon-deficient condition, for example inside water. The superhydrophobic surface has the contact angle 140°, while the superhydrophilic surface has the contact angle 25°. The untreated surface has the contact angle 60°.

The material classification was not provided. Therefore, energy-dispersive X-ray spectroscopy (EDS) was performed to determine the material. All the samples were analysed and it was found that these alloys contained 4.38–4.64 wt-% Mg, 0.26–0.40 wt-%Fe, 0.10–0.20 wt-%Cr, <0.14 wt-%Si, <0.10 wt-%Ti,<0.17 wt-%Cu and <0.20 wt-%Zn. After analysing the EDS results, the material used in this study was determined to be aluminium alloy 5083.

The samples were then imaged under an electron microscope to run a qualitative comparison of the surface topography between the three groups. Figure 1 shows three representative samples: (a) superhydrophobic, (b) superhydrophilic, and (c) untreated control samples. It appeared that the laser-treated surfaces were oxidised and there were holes created on the surfaces as can be clearly seen in the insets of Figure 1(a,b). The surface of the FLSP-treated samples showed the presence of oxide scale on the surface, while the untreated surface showed it to be a metallic surface. This is demonstrated in Figure 2 where the EDS spectra from

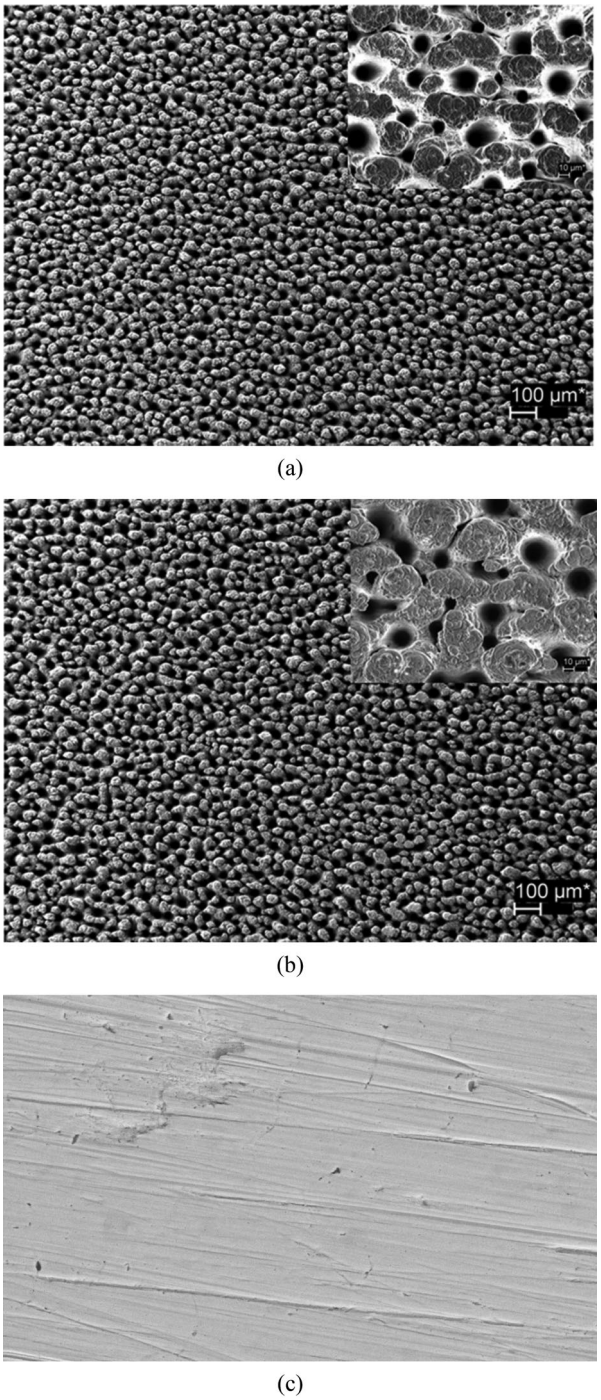

Figure 1. Secondary electron images from (a) Superhydrophobic, (b) Superhydrophilic, (c) Untreated.

these three samples are presented. One can see the high oxygen peak in the spectra from the superhydrophobic and the superhydrophilic surfaces, while that from the untreated alloy showed no substantial oxygen peaks at all. The superhydrophobic and the superhydrophilic sample surfaces show the presence of Si and P, respectively, and they are presumably from the surface treatment for obtaining the desired wettability characteristics and not associated with the laser treatment. The details of the surface treatment are not known to the authors. From the images examined, it was determined that the surface topography between the different FLSP samples were identical within the confines of a randomly generated self-organised below-surface growth. This further reinforces the ideas mentioned above. It is the treatment directly following laser texturing that determines wettability.

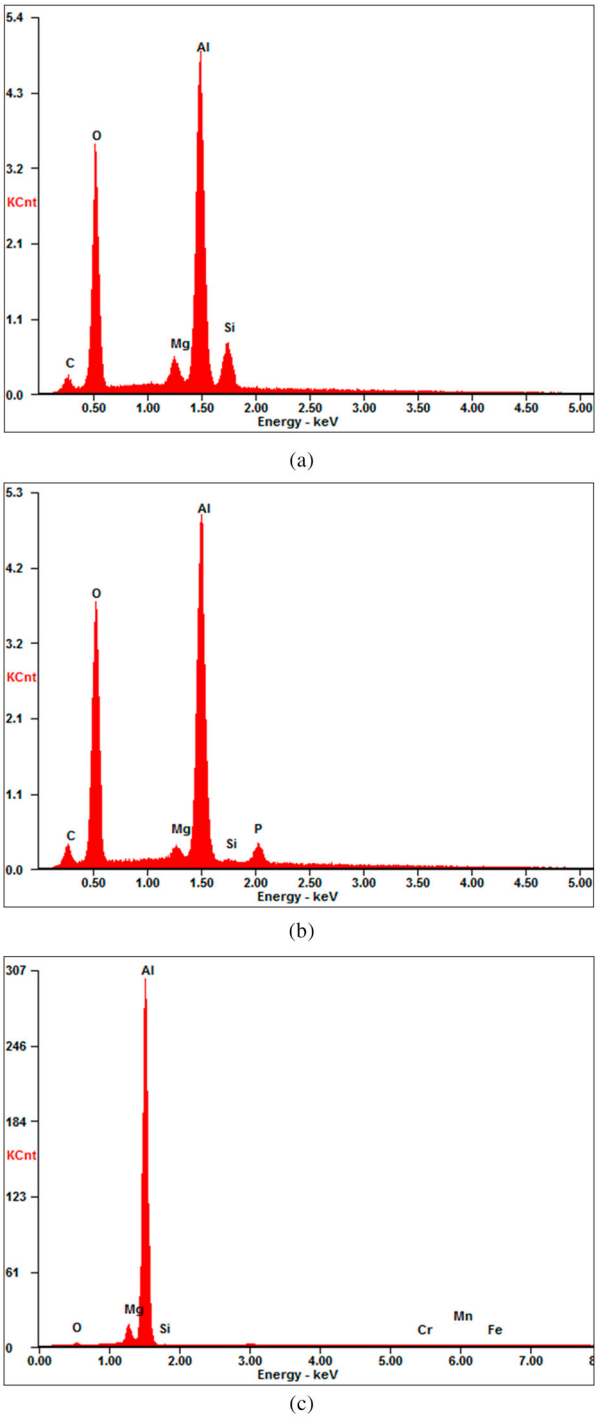

Figure 2: Energy-dispersive spectra from (a) Superhydrophobic, (b) Superhydrophilic, (c) Untreated.

Experimental set-up

Using an associated environmental systems salt fog chamber model MX-9204, 21 samples were suspended to a height of 50% of the total enclosure height and exposed to an atmosphere consisting of an atomised 3.5 wt-% sodium chloride salt solution and a temperature of 35°C. The samples were left in continuous contact with the atmosphere for 1000 h, with the exception of 1 h per week for observation and mass measurements. During the weekly observations, the surfaces of the samples were allowed to dry; however, no alterations were made. Each sample was suspended with a synthetic non-wicking material and aligned in three rows evenly spaced, each row consisting of superhydrophobic, superhydrophilic, and untreated samples. At the conclusion of the experiment, the samples were allowed to dry as normal for weight measurements and then cleaned with deionised water to remove excess salt deposits. Once the salt was removed, the samples were weighed a final time to obtain the overall weight difference.

Results and discussion

Throughout the corrosion test, multiple samples of the same material and surface treatment were tested in parallel to ensure that there were no anomalous findings. After the completion of testing, all samples within a group behaved in a similar manner, therefore, for brevity only one sample from each group is discussed here.

Visual observations

After the first week of continuous contact with a salt fog atmosphere, each sample from the three groups appeared to be wet. This was an expected result for the superhydrophilic and untreated sample, but was more of a surprise for the superhydrophobic sample. The first hypothesis is that the atomised water vapour is small enough in scale to penetrate the micro-scale surface features and bind to the metal substrate in areas of low density carbon. Figure 3 shows a superhydrophobic, superhydrophilic, and untreated sample directly after being removed from the fog chamber.

It should be noted that while storing the superhydrophilic samples prior to testing, contact was made with zinc oxide, giving a whitish appearance on the surface. It was decided to include these samples in the testing since zinc oxide is

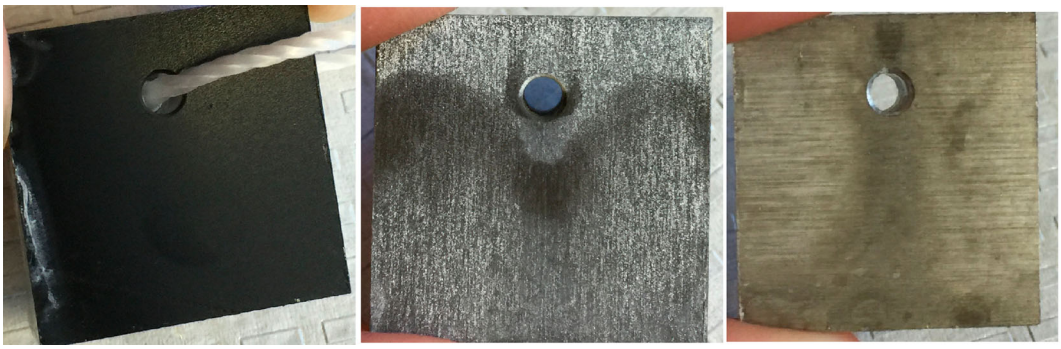

Figure 3. Corrosion Test Week 1, (L) Superhydrophobic, (M) Superhydrophilic, (R) Untreated.

nobler than aluminium, and the aluminium substrate will corrode preferentially to zinc oxide.

In week two, as illustrated in Figure 4, there is a significant accumulation of salt on the superhydrophobic sample, while the other two samples remain largely unchanged. Again, in week three, there is visual evidence of salt accumulation and distribution on the superhydrophobic sample, while the superhydrophilic and untreated samples remain mostly unchanged. While each sample pictured is of the same sample, opposite sides may be shown to illustrate an even presence of the findings seen for both sides of a sample. Figure 5 shows the samples after three weeks in the corrosion chamber.

In week four, significant changes and deviations begin to happen to the superhydrophobic sample compared to the other two. As seen in Figure 6, surface pitting begins to develop in areas of high salt concentration. These pits cause the removal of the functionalised surface leaving only the base material behind.

When examined under a microscope as seen in Figure 7, the evidence of salt accumulation and surface degradation on the superhydrophobic sample becomes quite clear. However, when examining the superhydrophilic sample, there is very little change, and almost no salt accumulation. The difference between superhydrophobic and superhydrophilic samples is quite vivid.

After week five, there is continued, rapid surface degradation of the superhydrophobic material, while again there is little change to the superhydrophilic material. Salt deposits begin to form on the untreated samples; however, there is no evidence of any pitting corrosion, as seen in Figure 8.

The final week sees progressed salt accumulation on all three sample groups. There is pronounced salt crystal growth on the superhydrophobic sample as well as continued rapid

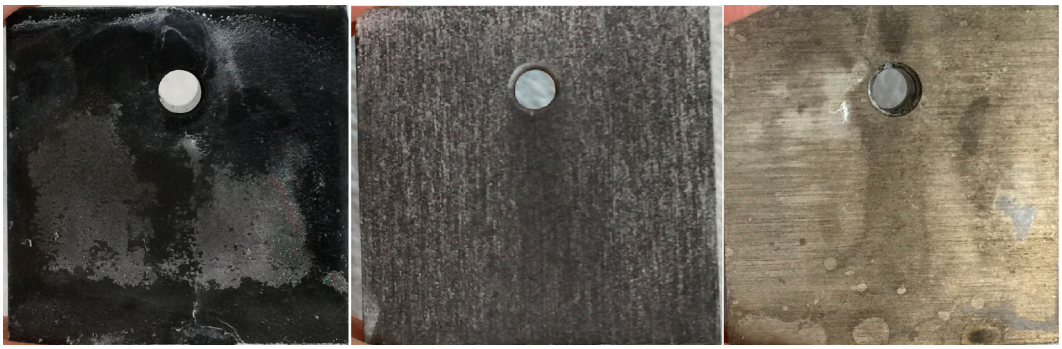

Figure 4. Corrosion Test Week 2, (L) Superhydrophobic, (M) Superhydrophilic, (R) Untreated.

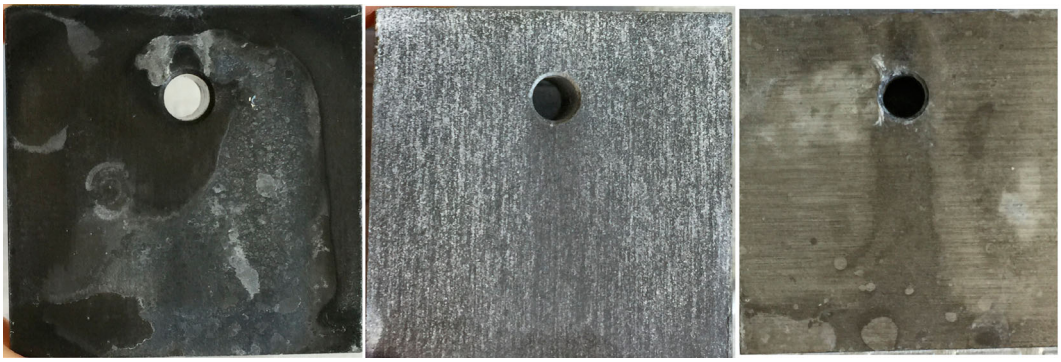

Figure 5. Corrosion Test Week 3, (L) Superhydrophobic, (M) Superhydrophilic, (R) Untreated.

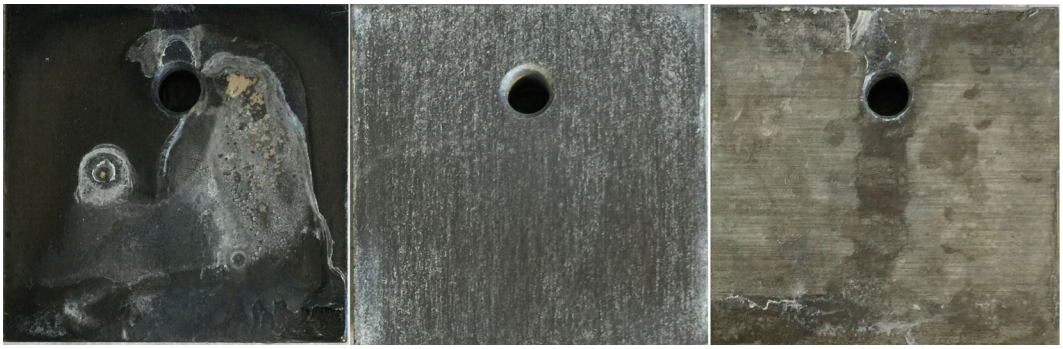

Figure 6. Corrosion Test Week 4, (L) Superhydrophobic, (M) Superhydrophilic, (R) Untreated.

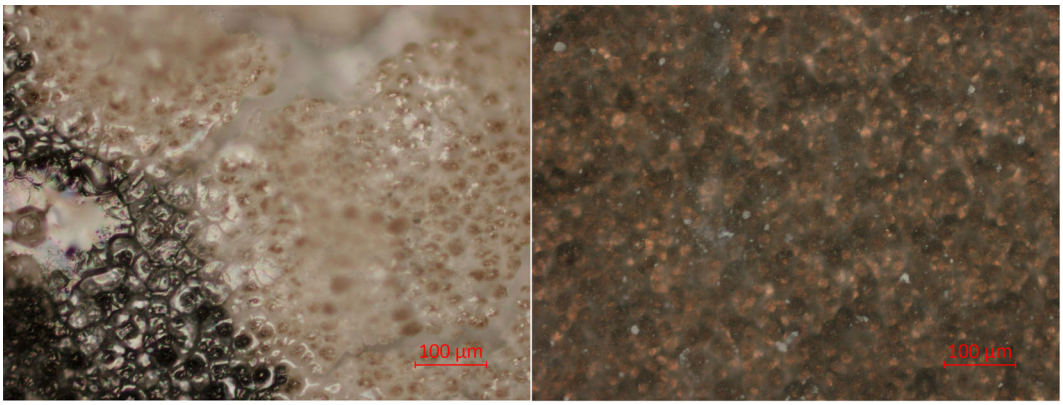

Figure 7. Corrosion Test Week 4 Magnified view, (L) Superhydrophobic, (R) Superhydrophilic.

degradation of the functionalised surface. The superhydrophilic sample begins to show crystal growth in the lower left corner along with some minor surface degradation. It should be noted that each sample has a thickness of 12.7 mm (0.5 in.) that is untreated bare metal. This surface on the bottom of the superhydrophilic sample was most likely the initiation point of the salt accumulation and not the functionalised surface itself. The untreated sample begins to show significant crystal growth; however, there is little evidence for pitting corrosion to have yet occurred. Figure 9 illustrates all these points.

When examined under a microscope, the accelerated corrosion rate suffered by the superhydrophobic material becomes quite evident. In Figure 10, the superhydrophobic sample on the left shows a large pit of exposed bare metal. The blurred image in the foreground is a growth of salt crystals on the original surface level. In contrast, the superhydrophilic sample shows very little salt embedded into the micro-structure of the surface. The untreated sample on the right is showing significant crystal growth on the surface; however, there is little sign of pitting. This would lead to the conclusion that functionalising a surface with superhydrophobic properties would ultimately increase the corrosion rate of the surface, limiting the resiliency of the material.

Mass measurement

Each week after visual observations, the mass of the samples was obtained following the removal of the non-wicking hanger and an appropriate amount of time for the samples to dry. The seventh week entry in the table are the mass measurements taken after the samples had been submersed in 95°C agitated deionised water for 30 min, and then allowed to dry for 1week, to facilitate the removal of salt from the samples. Figure 11 shows the mass data plotted over time for graphical comparison.

From the initiation of the test, each group of samples has an immediate gain in mass due to the deposition of salt. However, the magnitude of that deposition is greatly varied. In the first 2 weeks, as evidenced by the visual observations, the superhydrophobic sample has the greatest mass gain of 0.130% per 1 cm^2, while the superhydrophilic and untreated samples have mass gains of 0.065 and 0.070%, respectively. After week two, until the conclusion of the test, the superhydrophilic samples mass gain tapers off to a moderate rate with the peak mass gain of 0.087%. In contrast, the rate of mass gain for both the superhydrophobic and untreated samples increased with the peak mass gain of 0.430 and 0.324%, respectively. Despite the similar mass gain rates of the superhydrophobic and untreated samples, as the visual observations would suggest, the superhydrophobic sample suffered greater corrosion rates than the other samples.

These results showed that the weight change of the untreated and the superhydrophilic samples during the initial four weeks of the testing was similar, while that of the superhydrophobic sample was much higher. After four weeks, the weight change of the untreated and the superhydrophobic samples increased very rapidly, while that of the superhydrophobic sample was always higher. It appears from the increase in mass that the chloride salt deposition on the superhydrophobic samples is very high in comparison to the untreated and superhydrophilic surfaces. However after 4 weeks of tests, there is an increased rate of salt deposition

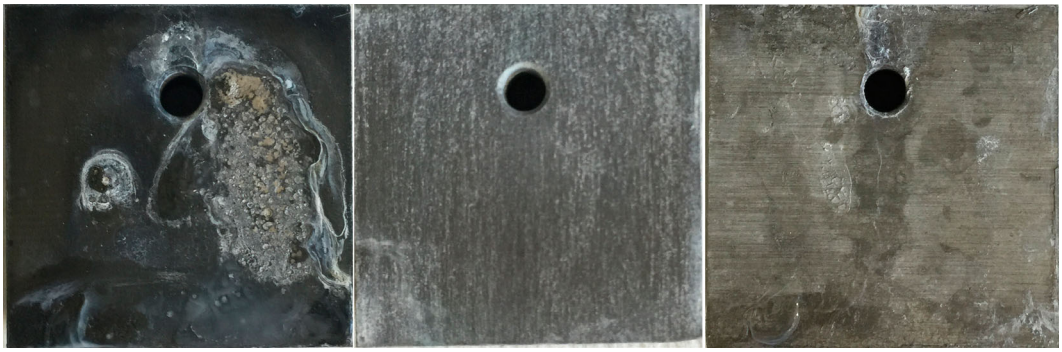

Figure 8. Corrosion Test Week 5, (L) Superhydrophobic, (M) Superhydrophilic, (R) Untreated.

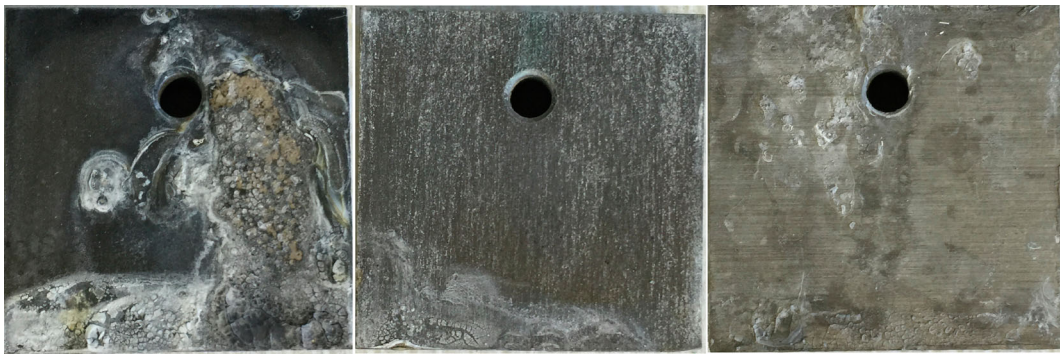

Figure 9. Corrosion Test Week 6, (L) Superhydrophobic, (M) Superhydrophilic, (R) Untreated.

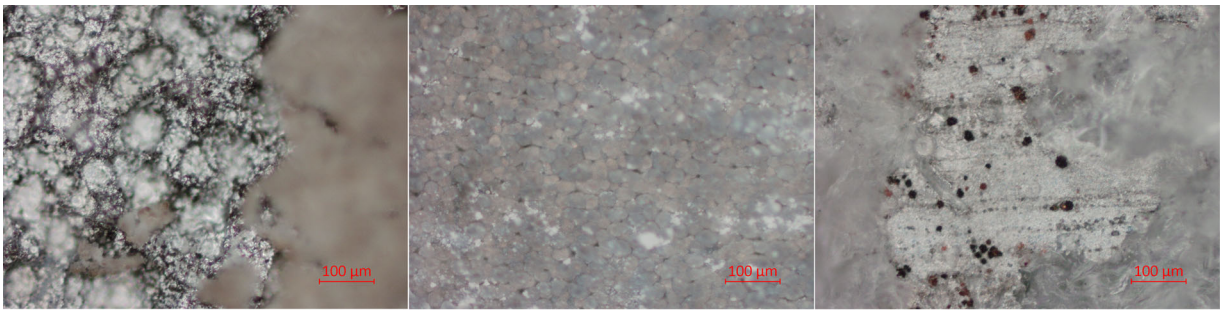

Figure 10. Corrosion Test Week 6 Magnified view, (L) Superhydrophobic, (M) Superhydrophilic, (R) Untreated.

on the untreated and the superhydrophobic samples. Towards the end of the test, by 7 weeks, understandably, the accumulated salt deposits lost their adherence to all the surfaces, easily removed to a great extent at the end of tests by the cleaning procedure mentioned earlier, and subsequently all samples show a weight decrease. The increased chloride concentration on the untreated and the superhydrophobic samples leads to an increased pitting corrosion of these samples by the breakdown of the protective alumina surface film. It is suggested that due to the superhydrophobic nature of the surface, polar water molecules are easily repelled enriching the surface with chlorides to a great extent. Clearly the superhydrophilic samples do not promote the increased chloride ion accumulation and thus presumably the native oxide is preserved on the surface. These observations are in conformity with the short-term exposure studies reported in earlier [10,11]. The fact that the superhydrophilic surfaces showed better corrosion resistance may be related to the presence of the phosphorus containing compound on the alloy surface, as phosphating or P-containing conversion coatings are known to improve the corrosion resistance of aluminium alloys [13,14].

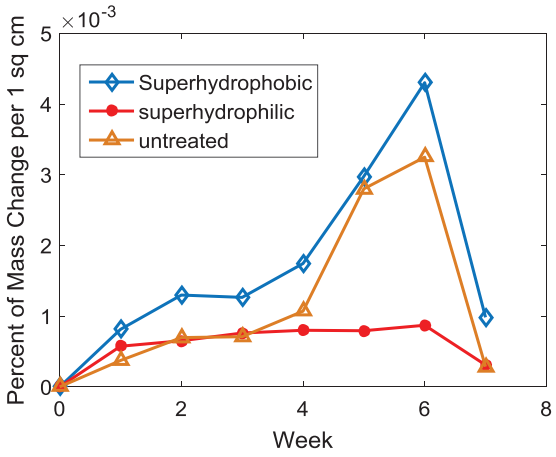

Figure 11. Sample mass change over time.

Conclusions

Superhydrophobic, superhydrophilic, and untreated samples were subjected to an accelerated corrosion test to gage the effect of surface processing on corrosion rates. Placed in an environment containing a 3.5% atomised salt solution held at 35°C for 1000 h, the conditions of the sample surfaces and sample masses were monitored weekly. It became clear early that functionalising a surface with superhydrophobic properties has a detrimental effect on corrosion resistance. The superhydrophobic sample exhibited an impressive salt retention capability over the other two samples, as well as rapid surface degradation through pitting corrosion. It appears that from a corrosion point of view, superhydrophilic surface may perform better than the untreated surface. At the conclusion of the test, the superhydrophobic sample showed the greatest mass gain, indicating a higher rate of corrosion when compared to the superhydrophilic and untreated samples.

While the hydrodynamic benefits of functionalising a surface with superhydrophobic properties were clear in a separate study, the decrease in corrosion resistance may offset any practical benefits of the material.

Acknowledgment

The team at the University of Nebraska-Lincoln (Drs Craig Zuhlke and Dennis Alexander) is appreciated for preparing samples using FSLP.

Disclosure statement

No potential conflict of interest was reported by the authors.

Funding

This research was sponsored by Office of Naval Research. The program manager is Ms Sarwat Chappell.

References

[1] Operation and maintenance overview fiscal year 2017 budget estimates (2016) Comptroller.defense.gov. [Online]. Available from: http://comptroller.defense.gov/Portals/45/Documents/defbudget/fy2017/fy2017_OM_Overview.pdf
[2] Wang W, Jiang L. Definition of superhydrophobic states. Adv Mater. 2007;19(21):3423–3424.
[3] Neinhuis C, Barthlott W. Characterization and distribution of water-repellent, self-cleaning plant surfaces. Ann Bot. 1997;79 (6):667–677.
[4] Chen W, Fadeev AY, Hsieh MC, et al. Ultrahydrophobic and ultralyophobic surfaces: some comments and examples. Langmuir. 1999;15(10):3395–3399.
[5] Krupenkin TN, Kolodner P, Taylor JA, et al. Turbulent drag reduction using superhydrophobic surfaces. Collection of technical papers: third AIAA flow control conference;2006 Jun 2006; San Francisco, CA.
[6] Daniello R, Waterhouse N, Rothstein J. Drag reduction in turbulent flows over superhydrophobic surfaces. Phys Fluids. 2009;21 (8):085103.
[7] Aljallis E, Sarshar MA, Datla R, et al. Experimental study of skin friction drag reduction on superhydrophobic flat plates in high Reynolds number boundary layer flow. Phys Fluids. 2013;25 (2):025103.
[8] Kietzig A, Hatzikiriakos S, Englezos P. Patterned superhydrophobic metallic surfaces. Langmuir. 2009;25(8):4821–4827.
[9] Zuhlke CA, Anderson TP, Li P., et al. Superhydrophobic metallic surfaces functionalized via femtosecond laser surface processing for long term air film retention when submerged in liquid. Proc. SPIE 9351, Laser-based Micro- and Nanoprocessing IX, 93510J, 2015 Mar, San Francisco, CA.
[10] Benedetti A, Cirisano F, Delucchib M, et al. Potentiodynamic study of Al–Mg alloy with superhydrophobiccoating in photobiologically active/not active natural seawater. Colloid Surface B. 2016;137:167–175.
[11] Boinovich LB, Emelyanenko AM, Modestov AD, et al. Synergistic effect of superhydrophobicity and oxidized layers on corrosion resistance of aluminum alloy surface textured by nanosecond laser treatment. ACS Appl Mater Interfaces. 2015;7:19500–19508.
[12] Zuhlke CA, Anderson TP, Alexander DR. Formation of multiscale surface structures on nickel via above surface growth and below surface growth mechanisms using femtosecond laser pulses. Opt Express. 2013;21(7):8460–8473.
[13] Pokhmurs'kyi VI, Kwiatkowski L, Zin IM, et al. Corrosion protection of aluminum alloys by inhibiting pigments. Mater Sci. 2006;42 (5):573–578.
[14] Ji S, Weng Y, Wu Z, et al. Excellent corrosion resistance of P and Fe modified micro-arc oxidation coating on Al alloy. J Alloys Compd. 2017;710:452–459.